J. Astron. Space Sci. 22(1), 47–58 (2005)

DEVELOPMENT OF ULTRA-LIGHT 2-AXES SUN SENSOR FOR SMALL SATELLITE

Su-Jeoung Kim[1,2†], Sun-Ok Kim[1,2], Byoung-Young Moon[1,2], Young-Keun Chang[1,2], and Hwa-Suk Oh[2]

[1]Space System Research Lab, Hankuk Aviation University, Goyang 412-791, Korea

[2]Department of Aerospace and Mechanical Engineering, Hankuk Aviation University, Goyang 412-791, Korea

email: mikeletto@hau.ac.kr

(Received September 20, 2004; Accepted January 26, 2005)

ABSTRACT

This paper addresses development of the ultra-light analog sun sensors for small satellite applications. The sun sensor is suitable for attitude determination for small satellite because of its small, light, low-cost, and low power consumption characteristics. The sun sensor is designed, manufactured and characteristic-tested with the target requirements of ±60° FOV (Field of View) and pointing accuracy of ±2°. Since the sun sensor has nonlinear characteristics between output measurement voltage and incident angle of sunlight, a higher order calibration equation is required for error correction. The error was calculated by using a polynomial calibration equation that was computed by the least square method obtained from the measured voltages vs. angles characteristics. Finally, the accuracies of 1-axis and 2-axes sun sensors, which consist of 2 detectors, are compared.

Keywords: ultra-light, field of view, analog sun sensor, micro/nano satellite

1. INTRODUCTION

The trend of satellite development is toward "Faster, Cheaper, Smaller, Better" satellite with miniaturization of electronic parts and circuits, and growth of integrated circuit technology from the 1990's. Many countries are focusing on developing small satellites such as microsatellite, nanosatellite, and picosatellite for the development of space technology with shorter production cycles. Currently various universities in different parts of the world are also developing nanosatellite and picosatellite for the satellite design discipline education purpose and verifying space technology in space environment (Kim & Chang 2003).

The satellite attitude determination and control system consists of actuators, sensors, and electronic controller assemblies. The sensor part measures the attitude information of a satellite which is important in performing the mission successfully. The sun sensor is popular, accurate, and reliable unit in spite of low power requirement and low mass for small satellite applications. It can be used for the normal attitude determination, the initial acquisition or failure recovery, or an independent solar array orientation determination system.

†corresponding author

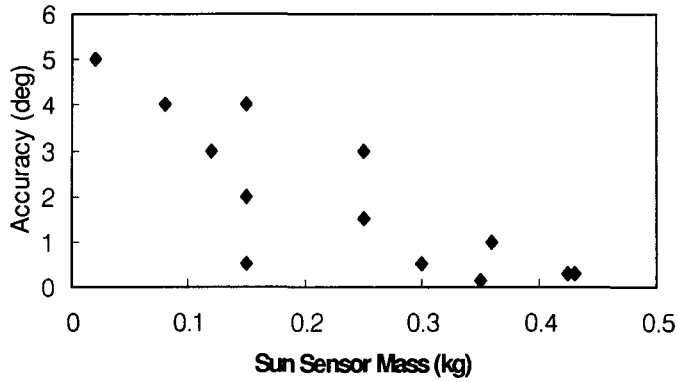

Figure 1. Mass vs. Accuracy of Analog Sun Sensors.

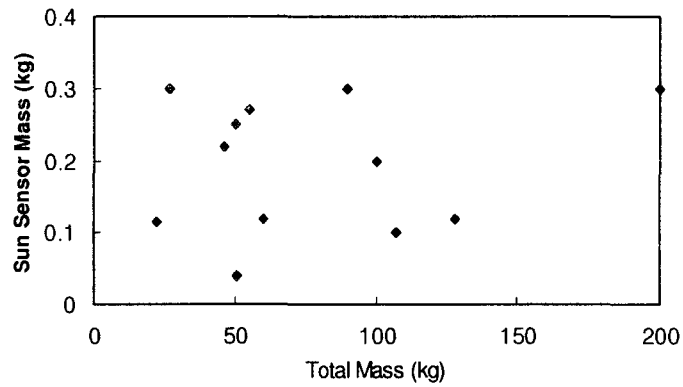

Figure 2. Sun Sensor Mass Distribution used for Small Satellite between 1990 and the Present.

The sun sensor is classified into analog and digital sensors according to type of detector and signal processing method. Figure 1 illustrates distribution of mass vs. accuracy of analog sun sensors used for small satellites from 1990 to the present. It can be seen that the mass of analog sun sensor is getting heavier as the accuracy increases. This study demonstrates how an ultra-light 1-axis and 2-axes analog sun sensors consisting of 2 detectors can be designed, manufactured and tested for small satellite applications. These sun sensors are developed based on the databases of various sun sensors implemented for small satellites since 1990s (Kim et al. 2004).

2. SUN SENSOR REQUIREMENTS

The main design parameters of the sun sensors for small satellite are mass, size and accuracy. Figure 2 presents the mass distribution of sun sensors used for small satellites between 1990 and the present. Figure 2 does not show a definite trend of sun sensor mass according to satellite mass. Figure 3 illustrates the size and height of sun sensor assembly modules used for small satellites between 1990 and the present. It is seen from Figure 3 that the minimum size was determined to be 60

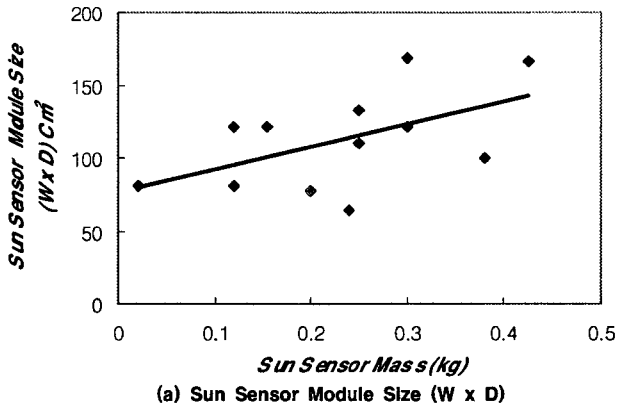

(a) Sun Sensor Module Size (W x D)

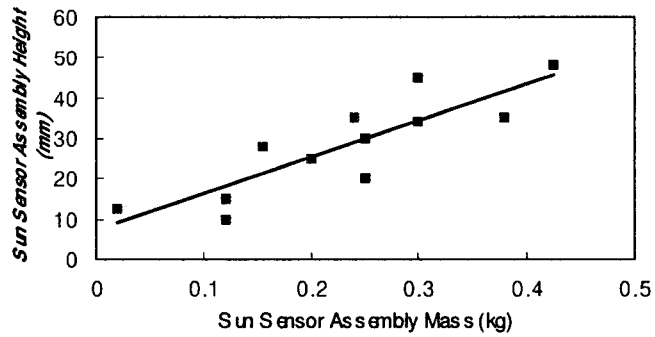

(b) Module Height

Figure 3. Sun Sensor Module Size and Height.

Table 1. Sun Sensor Requirements.

Parameter	Requirement
Size	$< 80 \times 80 \times 40 mm^3$
Mass	< 200 g
Accuracy	$< \pm 2°$

cm^2 and the maximum module height will be less than 50 mm for 2-axes sun sensors incorporating 2 detectors. Based on the database of the size and mass of sun sensors, the requirements of the sun sensor which we are developing have been established as shown in Table 1.

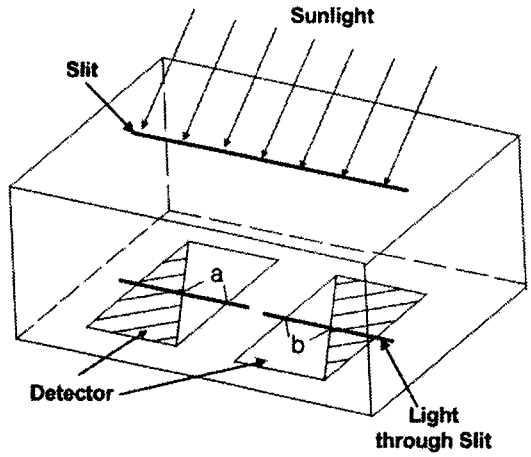

(a) Top View

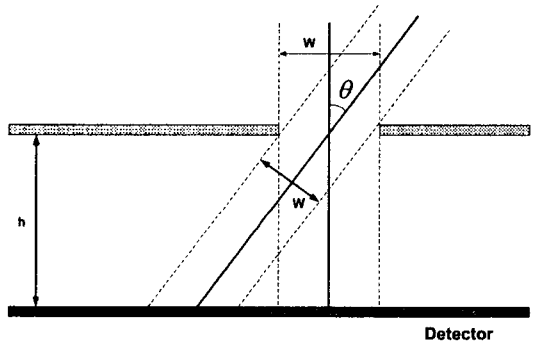

(b) Cross Sectional View

Figure 4. Configuration of the Sun Sensor.

3. ANALYSIS AND DESIGN OF SUN SENSOR

Figure 4a shows a simplified configuration of a sun sensor, which has two detectors and one slit, developed for small satellite applications. This configuration can be installed horizontally and vertically on a satellite, so that it can acquire 2-axes data for the satellite. The light through slit is projected onto two detectors and then the photo-current is generated, which is proportional to the length of sensor elements. The same amount of photo-current can be generated when the light is at a perpendicular incident. But, if the angle θ of the incoming light is inclined, there will be some differences corresponding to the difference between "a" and "b" as shown in Figure 4a.

The short-light-current, Isc of the detector is proportional to amount of irradiate light (Rhee et al. 1996).

$$\text{Isc} \propto (\text{length according to position}) \times (\text{a light quantity according to degree}) \quad (1)$$

Figure 4b shows that the light amount through the slit is changed depending on angles, and this can

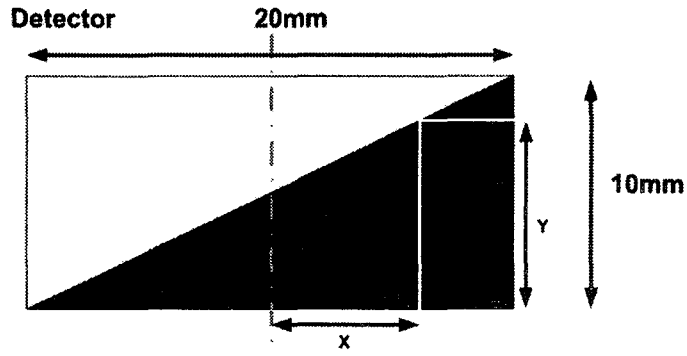

Figure 5. Configuration of Detector.

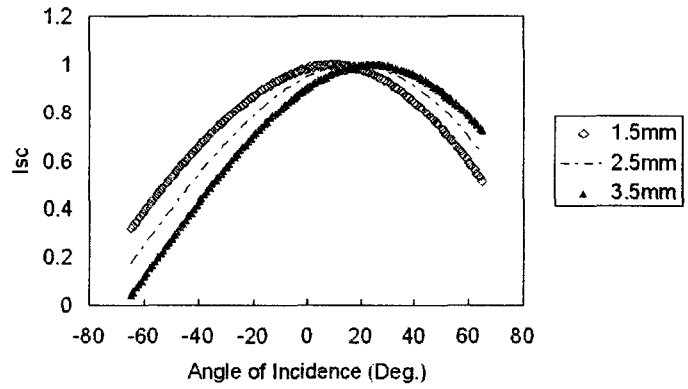

Figure 6. Change of Isc according to Angle of Incidence.

be described by equation (2) as follows:

$$s(\theta) = \omega \cos\theta \tag{2}$$

Where $s(\theta)$ is the amount of light, and ω is the slit width. The length of sun light is changed depending on the angles.

Figure 5 shows a configuration of a detector. Where x is the displacement of the center on the detector and y is the length depending on the angles. x is defined as shown in equation (3).

$$x = h \tan\theta \tag{3}$$

Where h is the length between the slit and the detector, and is defined by equation (4).

$$y(\theta) = 0.5(10 + h \tan\theta) \tag{4}$$

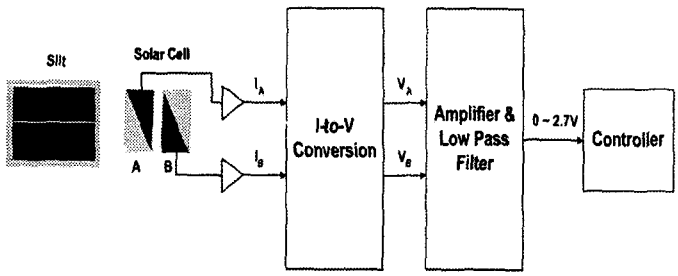

Figure 7. Block Diagram of 2 detectors Sun Sensor Made by SSRL.

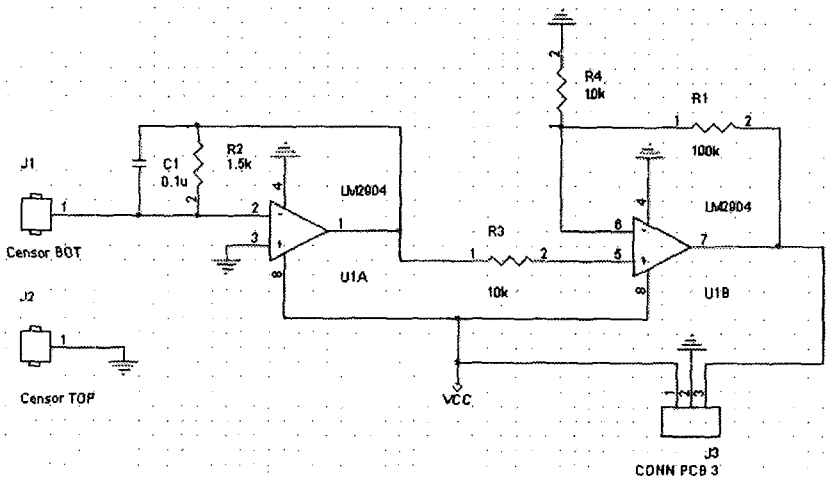

Figure 8. Circuits of 2 detectors Sun Sensor Made by SSRL.

Hence, the theoretical Isc of detector is given by equation (5).

$$\text{Isc} \propto y(\theta) \times s(\theta) = 0.5 \times \omega \times \cos\theta(10 + h\tan\theta) \tag{5}$$

Figure 6 shows variations in Isc depending on the incident angles for various h. The maximum position and width of Isc are varied for different h as shown in Figure 6. The slit width of 3.5 mm is suitable because it gives a wide range and large changes in Isc according to the incident angles. The output value of the detector does not mean real conversion of angles in the calculation. But, it illustrates a standard for appropriate operation of a manufactured sun sensor. The important factor is a relative response between two detectors (Chang et al. 1996).

The 2 detectors sun sensor consisted of a slit, 2 detectors, a circuit board, and a sun sensor box for integration. The circuit implements minimized mass and harness complexity in manufacturing ultra-light 2 detectors sun sensor. Figure 7 is a block diagram of the 2 detectors sun sensor. The output current from the 2 detectors is changed to voltage by I-to-V conversion. At this time, current

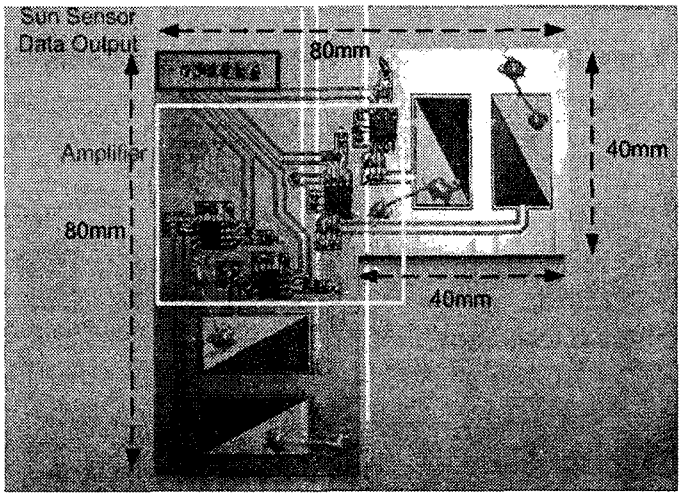

(a) Control Electronics of 2-axes Sun Sensor

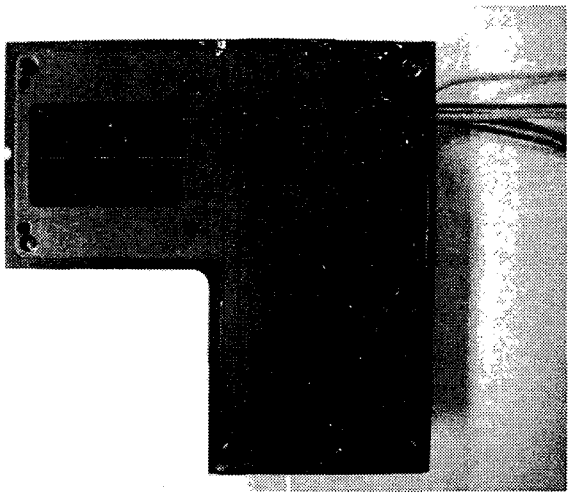

(b) 2-axes Sun Sensor Box

Figure 9. Prototype of 2-axes Sun Sensor.

to voltage converter must be incorporated so that the ratio of the current and voltage becomes 1:1. The changed voltage is amplified to 0 $\sim$ 2.7 V through amplifier. LPF (Low Pass Filter) reduces noise and high frequency. Figure 8 represents circuits of 2 detectors sun sensor developed for small satellite applications. Figure 9 shows a prototype of 2-axes sun sensor incorporating 2 detectors. Figure 9a is a control electronics of 2-axes sun sensor and Figure 9b is its sensor box, respectively. The size and mass of prototype sun sensor developed for small satellite applications is 80 $\times$ 80 $\times$ 30 mm and 150 g, respectively.

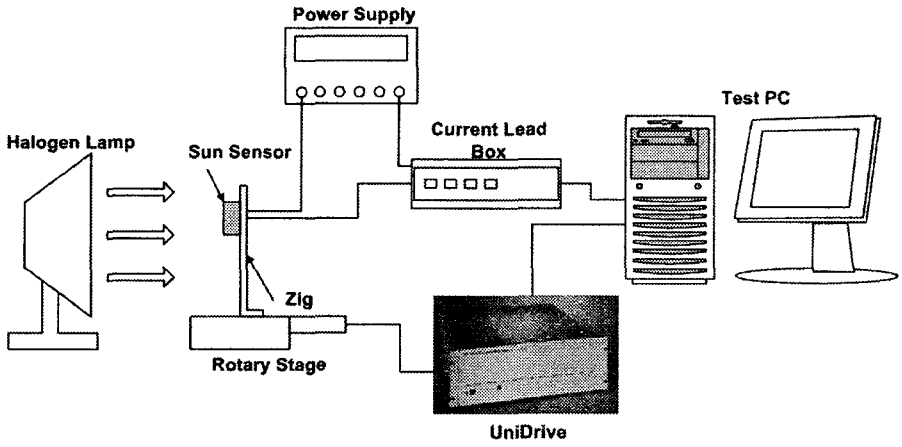

Figure 10. Test Diagram of Sun Sensor Characteristic Calibration.

4. SUN SENSOR CHARACTERISTIC TEST AND RESULTS

The characteristic testing of sun sensor requires light source, correction equipment for measurement, and optics table for accurate angle adjustment. For this measurement, the interval of measurement angle has been set up to be 1° using the rotary stage. Figure 10 shows test diagram of sun sensor. The sun sensor is installed on the zig and exposed to light source on the zig. The rotary stage is operated by UniDrive, which is connected with computer including motion controller. The measured output voltage is changed into digital signal through current lead box after it is stored in the PC (Kim 2004).

As mentioned above, the most important element during the characteristic test is that a dark room has to be provided to block off the light except one source of light. The zig and sun sensor box must be colored to black anodizing for the error cut-off from the reflection of light. Finally, the location of slit at the zig will be the center of rotary stage. If the slit isn't exactly positioned in the center, the detectors which are detecting light represent different attitude determination in the satellite. Figure 11a,b show test module attached in rotary stage and test configuration of sun sensor characteristics, respectively. The tests were performed for 1-axis and 2-axes sun sensors possessing 2 detectors to compare the accuracy.

4.1 Case 1: 1 axes (2 detectors) test results

Figure 12a shows output voltage of 1-axis sun sensor incorporating 2 detectors according to the angles of sunlight. This figure is similar to Figure 6. Figure 12b shows Va/(Va+Vb) according to the angle of incidence. Va and Vb are output voltage of cell a and cell b, as shown in Figure 6. It has excellent straight line with the exception of $\pm 40° \sim \pm 60°$. Figure 12c is compared data between the calibration and the correction values. There are various methods for the correction of a sun sensor (Wertz 1988). In this paper 3rd order line fitting algorithm was used among the various method. Figure 12c shows that the graph is approximated to output voltage rate p of the detector using 3th order polynomial. Equation (6) is a polynomial expression for the angle of incidence

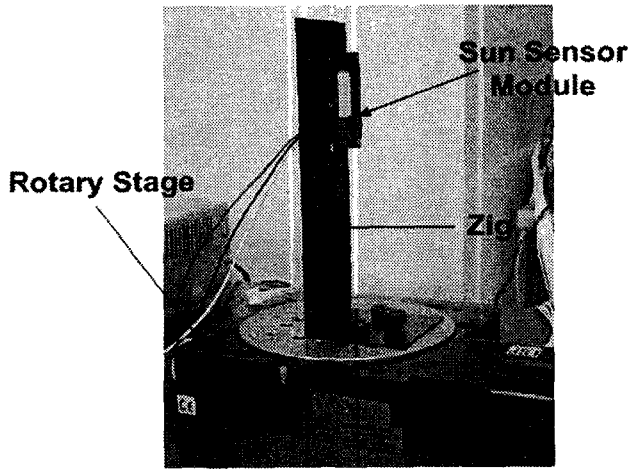

(a) Sun Sensor installed on Rotary Stage

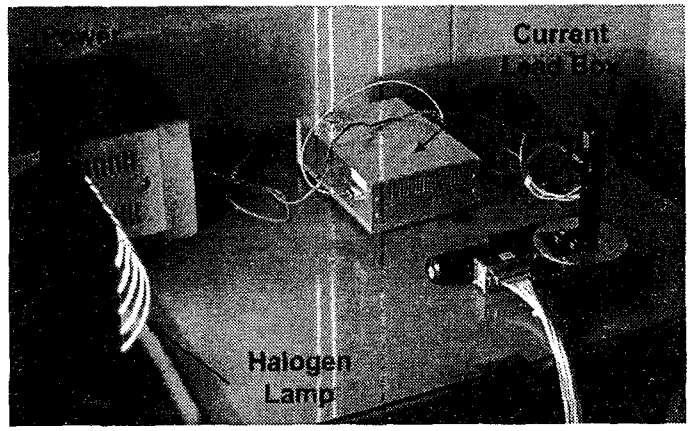

(b) Sun Sensor at Testing

Figure 11. Sun Sensor Characteristic Testing.

$(p = Va/(Va + Vb))$ (Ok 1993).

$$\text{Angle of incidence (deg)} = -4632.6p^3 + 6951.7p^2 - 2996.6p + 339.4 \quad (6)$$

Figure 12d shows the error between the calibration and 3rd order polynomial. As shown in Figure 12d, the error range is $+2.5° \sim -2°$. The accuracy of 1-axis sun sensor is approximated to be 0.988° by RMSE (Root Mean Square Error).

4.2 Case 2: 2-axes (2 detectors) test results

Figure 13a shows X-axis output voltage of 2-axes sun sensor according to angles of sunlight. Figure 13b shows Vx_a/(Vx_a+Vx_b) according to angle of incidence. It presents an excellent straight line. Figure 13c is compared data between the calibration and the correction values. There are various methods for the correction of sun sensor. Figure 13c shows that the graph is approximated

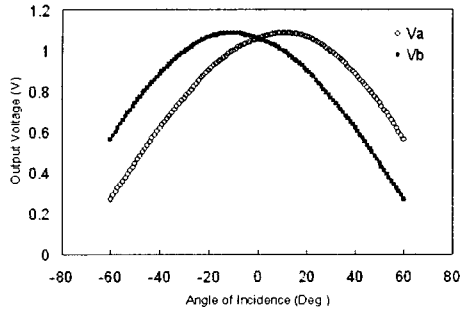

(a) Output Voltage according to Degree

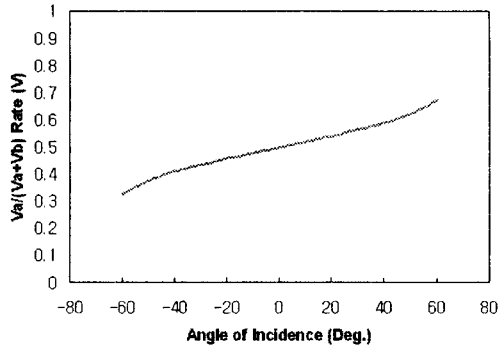

(b) Output Voltage Rate according to Degree

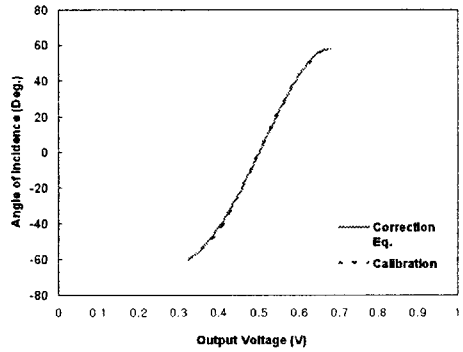

(c) Degree and 4th Order Polynomial according to Output Voltage Rate

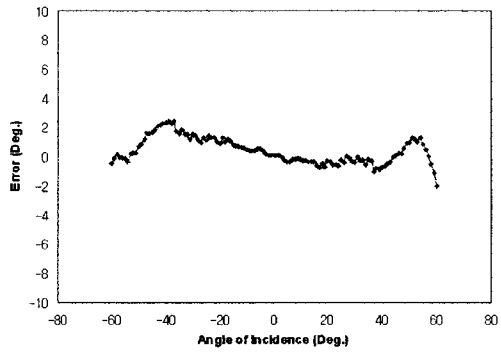

(d) Error Characteristic

Figure 12. Test Data in the 1-axis Sun Sensor.

to output voltage rate q of the detector using 3rd order polynomial. Equation (7) is a polynomial expression for the X-axis angle of incidence ($q = Vx\_a/(Vx\_a + Vx\_b)$).

$$\text{X} - \text{axis angle of incidence (deg)} = -12525q^3 + 18788q^2 - 8719q + 1228 \tag{7}$$

Figure 13d shows the error between the calibration and 3rd order polynomial. As shown in Figure 13d, the error range is $+1.8° \sim -2.1°$. The accuracy of X-axis in the 2-axes sun sensor is approximated to be 0.783° by RMSE (Root Mean Square Error). Figure 14a,b,c shows analysis of Y-axis output voltage. The data of Y-axis can be analyzed by the same method as X-axis. The Y-axis angle of incidence is approximated to output voltage rate r of the detector using 3th order polynomial. Equation (8) is a polynomial expression for Y-axis angle of incidence ($r = Vy_{-a}/(Vy_{-a} + Vy_{-b})$).

$$\text{Y} - \text{axis angle of incidence (deg)} = -1018.7r^3 + 1528r^2 - 476.1r - 16.6 \tag{8}$$

Figure 14d shows the error between the calibration and 3th order polynomial. As shown in Figure 14d, the error range is less than $\pm 2°$. The accuracy of Y-axis in the 2-axes sun sensor is 0.877° by RMSE. As shown in Table 2, the 2-axes sun sensor illustrates better performance than

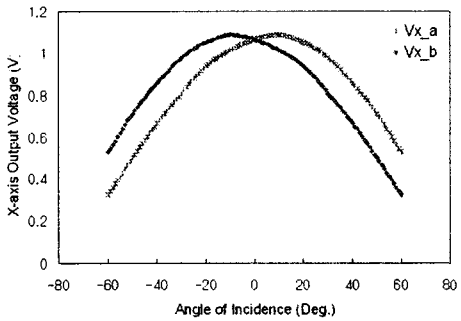

(a) X-axis Output Voltage according to Degree

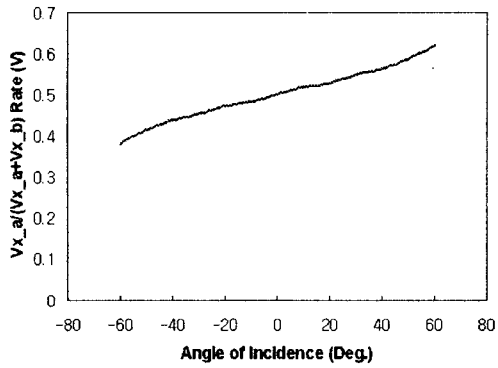

(b) X-axis Output Voltage Rate according to Degree

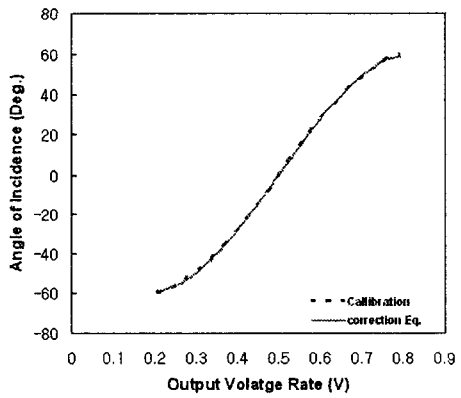

(c) Degree and 3th Order Polynomial according to X-axis Output Voltage Rate

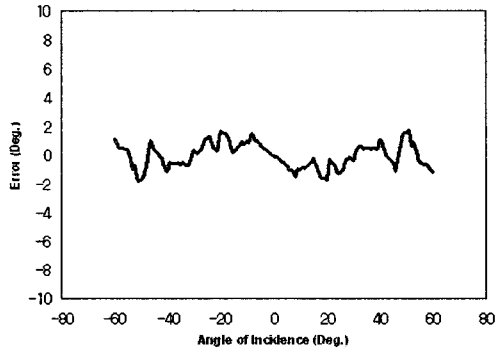

(d) X-axis Error Characteristic

Figure 13. X-axis Test Data in the 2-axes Sun Sensor.

Table 2. Accuracy Comparison of 1-axis and 2-axis Sun Sensor.

	1 Axes	2-Axis	
Accuracy	0.988°	X-Axis	0.783°
		Y-Axis	0.877°

1-axis sun sensor because the 2-axes sun sensor is affected less by diffused reflection. The 2-axes sun sensor satisfies the established requirements of error less than ±2°.

5. CONCLUSIONS

The ultra-light 1-axis and 2-axes sun sensors implementing 2 detectors have been designed and manufactured. The characteristic test has been conducted for the performance measurement. The 2-axes sun sensor developed here illustrates better performance than other analog sun sensors

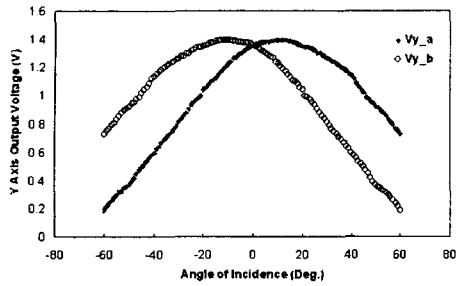

(a) Y-axis Output Voltage according to Degree

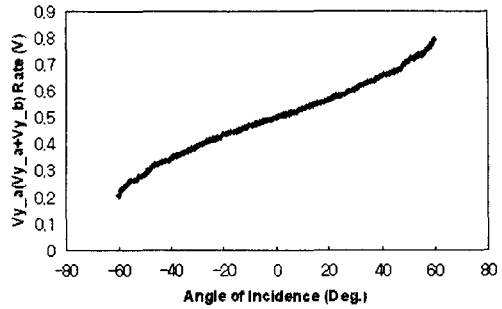

(b) Y-axis Output Voltage Rate according to Degree

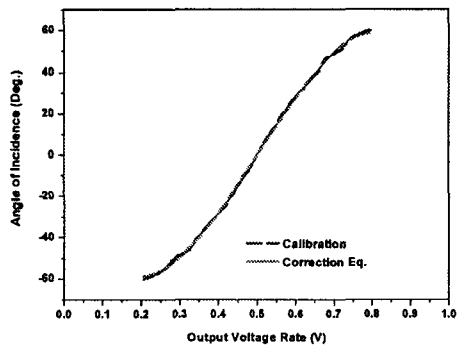

(c) Degree and 3th Order Polynomial according to Y-axis Output Voltage Rate

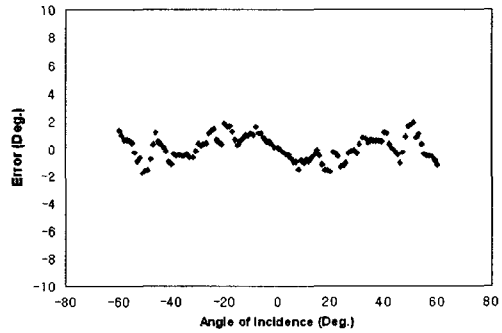

(d) Y-axis Error Characteristic

Figure 14. Y-axis Test Data in the 2-axes Sun Sensor.

with similar mass as shown in Figure 1. It can be seen that the 2-axes sun sensor developed at Space System Research Laboratory (SSRL) meets all of the requirements. The accuracy of 2-axes sun sensor is approximated to be 1.176° by RMSE. The accuracy can be improved through the implementation of an error reduction. The 2-axes sun sensor flight model will be manufactured for small satellite applications.

ACKNOWLEDGEMENTS: This study is supported by "Special Research Funding Program" awarded by Hankuk Aviation University. The authors wish to acknowledge the University's financial support.

REFERENCES

Chang, H. S., Kim, B. J., Lim, K. S., Sung, D. K., & Choi, S. D. 1996, JA&SS, 13, S173

Kim, S. J., Lee, M. H., & Chang, Y. K. 2004, in Proceedings of KSAS Spring Conference (Seoul: KSAS), p.860

Kim, S. O. 2004, MS Thesis, Hankuk Aviation University

Kim, Y. H. & Chang, Y. K 2003, in Proceedings of RAST (Istanbul: RAST), p.242

Ok, K. H. 1993, MS Thesis, Korea Advanced Institute of Science and Technology

Rhee, S. H., Lee, M. S., Lee, H. W., Lim, K. S., & Choi, S. D. 1996, JA&SS, 13, 254

Wertz, J. R. 1988, Spacecraft Attitude Determination and Control, ed. J. R. Wertz (Boston: Kluwer Academy Pub.), p.155